MALAYSIAN JOURNAL OF ANALYTICAL SCIENCES

Journal homepage: https://mjas.analis.com.my/

Research Article

D-optimal mixture design optimization of an oil-in-water nanoemulsion of *Pouteria campechiana* pulp extract and its physicochemical and stability properties

Roswanira Abdul Wahab[1,2*], Nur Haziqah Che Marzuki[1,2], Mariani Abdul Hamid[3], Norhayati Mohamed Noor[4] and Ni Made Suaniti[5]

[1] Department of Chemistry, Faculty of Science, Universiti Teknologi Malaysia, Skudai, Johor, Malaysia
[2] Investigative Forensic Sciences Research Group, Universiti Teknologi Malaysia, Skudai, Johor, Malaysia
[3]School of Chemical and Energy Engineering, Faculty of Engineering, Universiti Teknologi Malaysia, Skudai, Johor, Malaysia
[4] Cosmeceutical & Fragrance Unit, Institute of Bioproduct Development, Universiti Teknologi Malaysia, Skudai, Johor, Malaysia
[5] Department of Chemistry, Faculty of Mathematics and Natural Sciences, University of Udayana, Bali, Indonesia

*Corresponding author: roswanira@utm.my

Received: 14 October 2025; Revised: 1 March 2026; Accepted: 6 April 2026; Published: 30 April 2026

Abstract

The growing demand for cosmeceuticals is driven by rising awareness of the benefits of dermatologically active, natural ingredients and increasing concern over the toxicity of synthetic compounds. This study explores the untapped potential of *Pouteria campechiana* (Pc) fruit pulp as an active component in a nanoemulsion for topical application. Using the D-optimal mixture design (MD), formulation of the PC-based nanoemulsion was optimized for four components, namely, jojoba oil, grape seed oil, T80, and glycerol, to achieve minimal particle size and polydispersity index (PdI). The optimized formulation demonstrated excellent performance, with a particle size of 240.1 nm, PdI of 0.21, high model significance ($p < 0.0001$, $R^2 > 0.97$), and strong stability indicators: zeta potential of –33.6 mV, conductivity of 0.22 µS/cm, and no phase separation over 90 days of storage. Pertinently, the OPT-PcE-Ne demonstrated resilience in repeated ultracentrifugation and freeze-thaw tests, while maintaining a pH range suitable for topical skin application (4-6). No phase separation was observed in samples stored under varying temperatures for up to 90 days. Transmission electron microscope micrograph confirmed sub-250 nm droplet size, and Bingham plastic behavior further supports its topical cosmeceutical application. Hence, the optimized OPT-PcE-Ne formulation, utilizing Pc as a key active ingredient produced here, achieved optimal stability while possessing ideal characteristics for topical cosmeceutical uses. Additionally, the use of natural ingredients in the optimized OPT-PcE-Ne developed in this study presents a promising, safer alternative to synthetic skincare formulations.

Keywords: *Pouteria campechiana*, pulp extract, oil-in-water, D-optimal mixture design, nanoemulsion

Introduction

Pouteria campechiana, a member of the Sapotaceae family, is native to tropical and subtropical regions of Asia, including Sri Lanka and South Asia, as well as to Central and South America [1]. The species is known by various common names, such as 'canistel', 'egg-fruit', 'mammee sapote', and 'yellow sapote' in the Caribbean; 'Buah Kuning Telur' in Bahasa Melayu; and 'Sawo Mentega' in Indonesia. This tree requires a tropical or subtropical climate to flourish. In Guatemala, it is found at elevations up to 1,400 m, and in Florida, it can tolerate winter conditions as far north as Palm Beach and Punta Gorda, surviving in protected areas of St. Petersburg. *P. campechiana* thrives with moderate precipitation and is well-suited to regions with a prolonged dry season [2,3]. The fruit itself is characterized by a bulbous base, often featuring a 5-pointed calyx that may be rounded or form a distinct depression. It typically measures 7.5–12.5 cm in length and 5–7.5 cm in width. When unripe, the fruit has a green skin and a hard, gummy internal texture. Upon ripening, the skin becomes very smooth and glossy, turning a lemon-yellow, golden-yellow, or pale orange-yellow, occasionally marked with light-brown or reddish-brown russet (**Figure 1a-b**). Culturally, the fruit has long been valued for its

medicinal properties. In Mexico, it is believed to possess antipyretic qualities, while in Cuba, it is used to treat skin eruptions [4]. Despite these traditional uses and its potential benefits, *P. campechiana* remains underutilized.

The fruit's polyphenolic-rich extract shows promise as an active ingredient for topical nanoemulsions aimed at improving skin health. The antioxidant properties of its polyphenols help neutralize free radicals, which are known to cause progressive skin damage. Furthermore, Pouteria species are known for their rich triterpenes and flavonoids. Specifically, the methanolic extract of *P. campechiana* contains compounds such as gallic acid, (+)-gallocatechin, (+)-catechin, (-)-epicatechin, (+)-catechin-3-O-gallate, dihydromyricetin, and myricitrin, along with high levels of polyphenols [5]. These compounds exhibit significant radical-scavenging activity. Notably, proanthocyanidins, a class of polyphenols present, are known for their excellent antioxidant properties [6]. Collectively, these compounds may provide substantial protection against the damaging effects of reactive oxygen species and free radicals (**Figure 2**).

The growing consumer demand for natural, safe skincare has intensified interest in plant-derived cosmeceuticals [7]. This study proposes a novel nanoemulsion utilizing polyphenolic-rich *Pouteria campechiana* pulp extract, an underutilized fruit with considerable potential for cosmetic applications. The potential of *P. campechiana* is substantiated by both ethnobotanical evidence and its phytochemical composition, namely, its antioxidant-rich phytochemical profile and documented traditional applications that align with modern cosmeceutical needs. Traditionally used in Cuba to treat skin eruptions [4], the fruit contains bioactive compounds, including gallic acid, catechins, and myricitrin, all of which are recognized for antioxidant, anti-inflammatory, and skin-protective properties [5,6]. These offer natural alternatives to synthetic ingredients associated with carcinogenicity and endocrine disruption [8]. The species thrives in tropical regions across Asia and South America, with cultivation feasible up to 1,400 m and tolerance to dry seasons. Its substantial size (7.5–12.5 cm) and low water requirements support commercial viability in Malaysia and Indonesia, whose climates are similar to those of South America, where year-round harvesting is achievable. Notably, this study employs a systematic D-optimal mixture design, enabling efficient optimization with minimal experimental runs. Moreover, the use of these abundantly available, natural excipients further enhances formulation scalability and commercial relevance [4]. This integrated approach establishes a scientifically validated foundation for transforming *P. campechiana* into a sustainable, high-value cosmeceutical ingredient.

To formulate an effective topical nanoemulsion (Ne), it is crucial to optimize the composition of water, surfactant, and active ingredients. Edible solvents like grapeseed oil, fatty acids, and vitamins are ideal components for Ne formulations [9]. Non-ionic surfactants are preferred for Ne systems because they are less hazardous than ionic surfactants and have a lower critical micelle concentration, which enhances the in vivo stability of oil-in-water (o/w) emulsion dosage forms [10]. Additionally, the formulation technique plays a key role in creating nano-sized droplets containing the active ingredients. High-energy techniques, often combined with low-energy methods, are effective in producing nano-sized droplets. Notable high-energy techniques, including ultrahomogenization, high-pressure homogenization, and ultrasonic bombardment, are typically used in formulating nanoemulsions [11-12].

(a) (b)

Figure 1. The a) *Pouteria campechiana* tree and b) mature fruits.

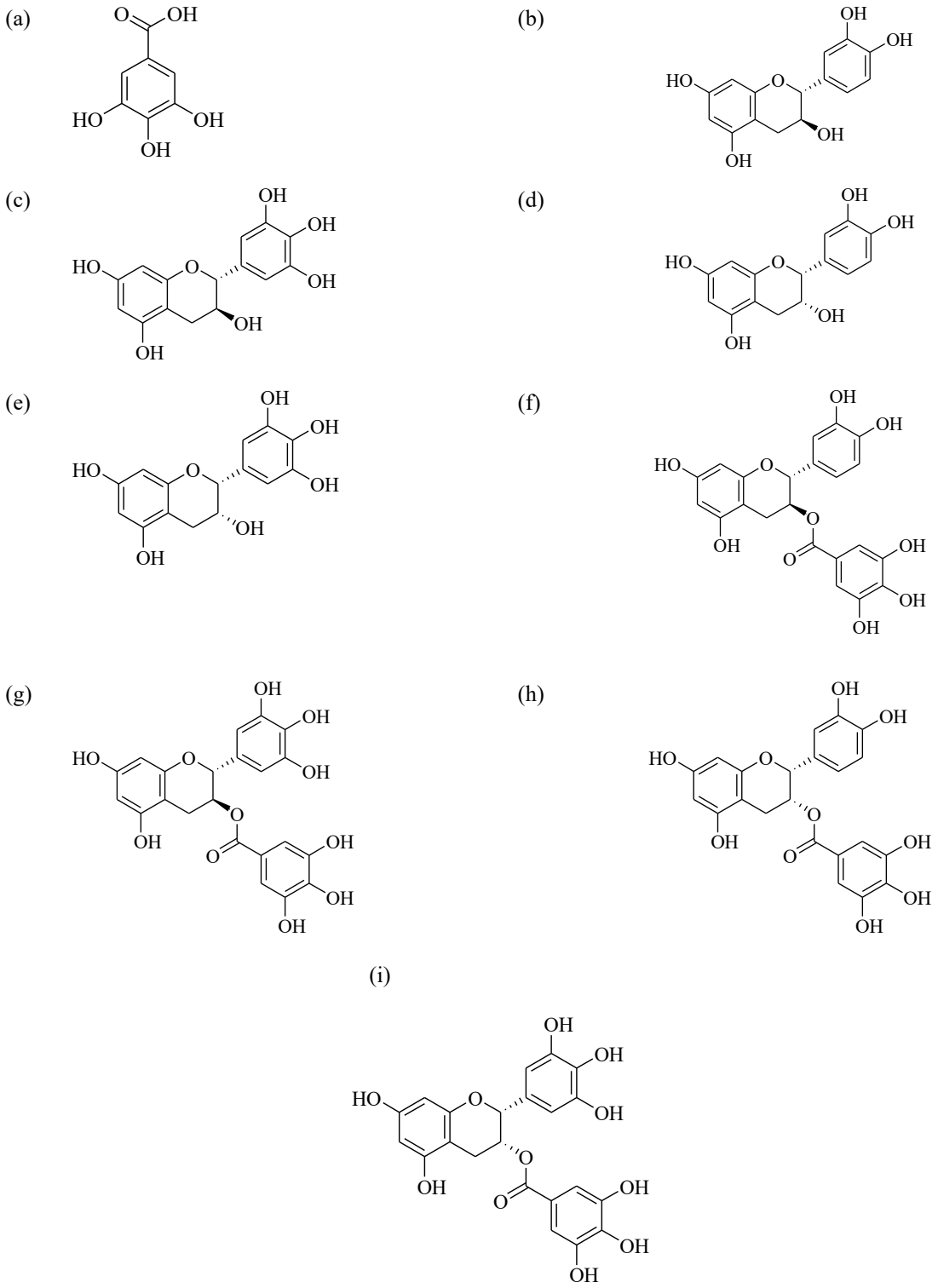

Figure 2. The bioactive compounds (a) gallic acid, (b) catechin, (c) gallocatechin, (d) epicatechin, (e) epigallocatechin, (f) catechin gallate, (g) gallocatechin gallate, (h) epicatechin gallate, (i) epigallocatechin gallate, are found in the *P. campechiana* pulp.

This study aims to harness the untapped polyphenolic and antioxidant potential of *P. campechiana* pulp extract to develop an optimized oil-in-water nanoemulsion for topical cosmeceutical applications. While *P. campechiana* has been traditionally used for skin-related applications and its phytochemical profile is well-documented, no study to date has systematically formulated its pulp extract into a stable nanoemulsion for topical cosmeceutical use. This work addresses this gap by employing D-optimal mixture design to optimize and characterize a P. campechiana nanoemulsion, thereby providing the first evidence-based framework for its incorporation into natural skincare products. Herein, the mixing protocol for its formulation combined hot-hot mixing, ultrasonication, and high-speed homogenization. The composition of the OPT-PcE-Ne was optimized using the D-optimal mixture design (MD), a multivariate statistical approach well-suited for experimental designs with multiple constraints and fewer optimization trials [13]. Moreover, the D-optimal MD has been successfully applied in several studies to identify optimal compositions for drug delivery and cosmetic applications [14-15]. The optimized parameters for the OPT-PcE-Ne formulation include the concentrations of Jojoba oil, Grapeseed oil, T80, and glycerol, with the goal of achieving the smallest particle size and the lowest polydispersity index (PdI). The optimized formulation was also evaluated for stability under varying temperature conditions, and its physical, organoleptic, and thermodynamic properties were elucidated. While *P. campechiana* has been traditionally used for skin-related applications and its phytochemical profile is well-documented, no study to date has systematically formulated its pulp extract into a stable nanoemulsion for topical cosmeceutical use. This work addresses this gap by employing D-optimal mixture design to optimize and characterize a *P. campechiana* nanoemulsion, thereby providing the first evidence-based framework for its incorporation into natural skincare products. By employing a D-optimal mixture design to minimize particle size and polydispersity while ensuring long-term stability, this work addresses the growing demand for natural, non-toxic skincare alternatives, offering a sustainable formulation comprising the *P. campechiana* extract as a natural alternative ingredient that could mitigate risks posed by synthetic chemicals and support the large-scale utilization of underutilized tropical fruits.

Materials and Methods

Materials

The ripened *P. campechiana* fruits (Pc) were collected from Nasuha Herbs and Spices (2° 2' 21.38" N latitude, 102° 34' 8.7" E longitude) in the Pagoh area of Johor, Malaysia, and biologist, Dr. Mohd Firdaus Ismail, validated the plant. The voucher specimen (MFI 0058/19) was deposited at the Institute of Bioscience, Universiti Putra Malaysia. Jojoba oil from Simmondsia chinesis was purchased from Sigma-Aldrich (St. Louis, USA), while the grapeseed oil was purchased from Borges (Catalonia, Spain). Surfactant T80 was purchased from Scharlau (Barcelona, Spain). Other chemicals, such as glycerol, were also acquired from Sigma-Aldrich (St. Louis, USA). Cosmeceutical grade T80 (T80) and xanthan gum (XG) were procured from Personal Formula Resources (Selangor, Malaysia), while cosmetic grade phenoxyethanol was purchased from Nacalao Tesque (Japan). Deionized water was purified using the MilliQ Direct 8 water system (Merck KGaA, Darmstadt, Germany).

Preparation of *P. campechiana* pulp extract (PcE)

The Pc fruits were cleaned under running tap water, and only the pulp was collected for subsequent drying. A 300 g sample of the pulp was oven-dried at 50 °C for 24 h, then ground into powder using a standard blender. The powdered Pc sample was packed in a polyethylene bag and stored at −10 °C. The Pc pulp was extracted using a Soxhlet apparatus for 24 h, using petroleum ether (30−60 %) as the solvent. The obtained crude extract was a relatively viscous yellow liquid with an orange-colored resin-like precipitate. The sample was then vacuum evaporated and stored at −10 °C until further use.

Screening the composition of *P. campechiana* pulp extract nanoemulsion

Formulation of the OPT-PcE Ne used an integrated hot-hot process followed by high-shear homogenization. To ensure that variations in particle size were attributable solely to compositional changes, the emulsification process itself was rigorously standardized across all formulations. Parameters including ultrasonication time (150 s), high-speed homogenization speed and duration (20,000 rpm for 5 min followed by 10,000 rpm for 5 min), and temperature (maintained between 45-60°C) were held constant. This fixed energy input ensures that the observed differences in particle size (Section 3.2, Table 2) are directly attributable to the mixture components (Jojoba oil, GSO, T80, Glycerol) and their interactions, as modeled by the D-optimal design. The oil and aqueous phase pre-mix emulsions were prepared in the required amounts and were heated at 60 °C. First, the surfactant mixture (glycerol and T80) was ultrasonicated for 150 s, and the same process was repeated for the oil mixture (JO and GSO). Appropriate amounts of water were heated to 60 °C, then the Pc extract was added while stirring at 300 rpm for 5 min. The surfactant mixture was added to the aqueous mixture and stirred for 5 min. Then, the oil mixture was added to the aqueous mixture with stirring for a further 5 min at 500 rpm, followed by the addition of xanthan gum. The two phases were emulsified by stirring at 45−50 °C for 5 min, followed

Table 1. The independent factors for the 20-run Mixture Design (MD) to identify the optimal OPT-PcE-Ne

Variables	Level of Variables	
	Low	High
A: Jojoba oil (JO)	6.25	18.75
B: Grapeseed oil (GSO)	31.25	43.75
C: Tween 80 (T80)	4.69	14.06
D: Glycerol (GLY)	35.94	45.31

by ultrahomogenization using a high-speed homogenizer (Ultra-Turrax, T18 Basic, IKA, Germany) at 20,000 rpm for 5 min and at 10,000 rpm for 5 min. The preservative phenoxyethanol and the fragrance were added just before homogenization. The OPT-PcE-Ne was stored in scintillation bottles for further analysis.

Optimization of *P. campechiana* pulp extract nanoemulsion by D-optimal mixture design (MD): Model fitting and analysis of variance (ANOVA)

A four-factor D-optimal mixture design (MD) was employed in this study to assess the impact of Jojoba oil (A), GSO (B), T80 (C), and glycerol (D) on the particle size and PdI values of the OPT-PcE-Ne formulation. The D-optimal MD approach is ideal for optimizing factors when experimental responses depend solely on the proportions of the mixture ingredients [16]. Notably, the three best formulations, exhibiting the lowest particle size and PdI, were selected for subsequent zeta potential analysis. Literature has shown that stable nanoemulsions typically exhibit zeta potentials above +30 mV or below -30 mV, indicating high stability. These values suggest a sufficient energy barrier between dispersed droplets, preventing coalescence and ensuring prolonged suspension [17].

Table 1 lists the independent factors for the 20-run Mixture Design (MD) model used to formulate the optimal OPT-PcE-Ne. The lower and upper levels for each independent factor (**Table 1**) were established through preliminary formulation screening and informed by literature precedents, ensuring that the selected ranges would yield stable nanoemulsions while allowing meaningful optimization within the D-optimal design constraints. The design matrix was generated using Design-Expert 7.0.0 software (Stat-Ease Inc., Minneapolis, USA). The factors, A (Jojoba oil), B (Grapeseed oil), C (T80), and D (glycerol), were evaluated at high and low levels, with their sum fixed at 100%. Each design was assessed individually to determine the influence of each factor on the responses. To evaluate the model's fitness, statistical significance was assessed using Fisher's F-test and the p-value. The F-value is the ratio of the model's mean square to the residual error mean square, indicating the model's significance and the magnitude of the factors' influence on the responses (PdI and particle size). A high F-value and low p-value suggest the model is significant, with independent factors having a strong impact on the responses. A p-value of < 0.05 is considered statistically significant. Additionally, other parameters such as the coefficient of determination (R^2), adjusted R^2 (R^2adj), adequate precision, lack of fit, and coefficient of estimation were used to evaluate the model's quality.

Statistical analysis

Next, the effect of study factors on the nature of prepared OPT-PcE Ne was assessed. Analysis of variance (ANOVA) was performed on the MD to assess significant differences among the independent variables. The experimental data were analyzed using a reduced model ($p < 0.05$) and multiple regression.

Model verification

A few random formulations were prepared based on the final MD results to validate the model predictions and assess the suitability of the reduced final model. The percentage prediction error (PPE) was calculated for each response: particle size and PdI. The sample with the lowest PPE value, calculated using Equation (1), was selected as the optimized OPT-PcE Ne. The calculation was germane to this study for assessing the adequacy of the final reduced model.

Results and Discussions

Screening factors

A preliminary screening study was conducted to establish feasible ranges of composition for the four independent factors prior to D-optimal optimization. The objectives were to: (1) identify concentration boundaries within which stable nanoemulsions could be formed, (2) determine practical constraints imposed by each component's physical properties, and (3) ensure sufficient response variation for meaningful optimization. Fifteen trial formulations were prepared with varying compositions of JO (4-20%), GSO (20-50%), T80 (3-16%), and GLY (20-50%), while maintaining constant XG (2%) and water (33%). To maintain consistency, xanthan gum was kept constant at 2%, and water was fixed at 33% throughout the design, while the concentrations of JO, GSO, T80, and GLY were varied (**Table 1**). These composition ranges

were chosen based on preliminary study results that highlighted the optimal experimental conditions. It is pertinent to note that our formulations were assessed for initial stability (24 h), particle size, and visual appearance. The lower limit for JO (6.25%) was established based on observations that concentrations below this threshold resulted in insufficient oil phase volume to adequately solubilize the Pc extract, while the upper limit (18.75%) was constrained by jojoba oil viscosity (~45 cP at 25°C), which produced excessively viscous emulsions at higher concentrations. For T80, the lower limit (4.69%) represented the minimum surfactant concentration required to prevent phase separation within 24 h, while the upper limit (14.06%) was set below concentrations where excessive micelle formation could compete with droplet stabilization [18]. Glycerol limits (35.94-45.31%) were determined based on sensory evaluation, with the lower limit representing the minimum perceptible moisturizing effect and the upper limit constrained by formulation tackiness [19, 20]. In short, the selected ranges yielded nanoemulsions with particle sizes of 280-420 nm and PdI values of 0.18-0.44, providing an appropriate design space for subsequent optimization.

Optimization of *P. campechiana* pulp extract nanoemulsion by D-optimal mixture design: Model fitting and ANOVA

This study evaluated four key variables influencing the particle size (Y1) and PdI (Y2) of the PcE nanoemulsion: JO (A), GSO (B), T80 (C), and glycerol (D). The square terms A^2, B^2, C^2, and D^2 represent the squared effects of the respective independent variables on the responses. It is important to note that the squared terms are unrelated to concentration, and their effect remains consistent regardless of their square [21]. The results showed that the most significant factor influencing particle size (Equation 1) was factor A (Jojoba oil) (537.37A), followed by D (glycerol) (554.86D), B (GSO) (453.70B), and C (T80) (360.77C). It is found that all two-factor interaction terms (AB, AC, AD, BC, BD, CD) have negative coefficients (-203.72, -775.98, -369.16, -643.83, -478.35, -806.61), and only the three-factor interaction term (ABD) has a positive coefficient (+3448.89). Meanwhile, for PdI (Equation 2), the largest effect was observed with factor D (glycerol) (28.65D), followed by C (T80) (27.79C), B (GSO) (15.97B), and A (Jojoba oil) (13.41A). All two-factor interaction terms have negative coefficients (-59.16 to -114.92), and conversely, all three-factor and four-factor interaction terms have positive coefficients (+138.23 to +202.18). This is precisely what we observed in our optimization, in which the smallest particle size was achieved when JO was low (6.25%), and GSO was relatively high (~38-44%). Likewise, a low PdI was achieved when T80 was high (14%), and JO was low (6.25%).

Interestingly, no synergistic effects between the interacting factors were found for either response (particle size or PdI), as all interaction terms (AB, AC, AD, BC, BD, and CD) were negative. These negative interaction coefficients observed here indicate that the factors are interacting antagonistically. This, however, does not indicate a lack of correlation, but simply means that the combined effect of the two factors on the response is less than the sum of their individual effects. Therefore, to minimize particle size or PdI (our optimization goals), these factors should be set at opposite ends of their ranges (one high, one low) [11]. Furthermore, the particle size was more strongly influenced by the factors, as reflected by the larger coefficients (554.86 – 360.77) in Equation 1 compared to the PdI coefficients (28.65 – 13.41) in Equation 2. For PdI in Table 3(b), all interaction terms are significant ($p < 0.05$), reinforcing that the same parameters strongly influence droplet uniformity, a related aspect of the emulsion process. This consistency across responses validates the relevance of the parameters.

Hence, the predominance of antagonistic two-factor interactions in our system can be explained by the physical chemistry of emulsion formation. For the JO and T80 (AC term, -775.98): JO is viscous (~45 cP), while T80 reduces interfacial tension. When both are high, the viscosity increase from JO counteracts the droplet size reduction from T80, resulting in an antagonistic effect. In the case of GSO and GLY (BD term, -478.35), GSO reduces oil phase viscosity, while GLY increases aqueous phase viscosity. Their effects on droplet size during homogenization oppose each other. For the T80 and GLY (CD term, -806.61), both factors affect interfacial properties, but through different mechanisms (T80 at the interface, GLY in the bulk phase). Their combined effect on droplet size is less than the sum of their individual effects. This is consistent with the principle that in mixture systems, components often compete for interfacial space or have opposing effects on physical properties, leading to antagonistic interactions [22, 23]. Hence, the D-optimal design empirically determines these interactions, enabling identification of the optimal balance point where antagonistic effects are minimized.

$$\text{Particle Size (Y1)} = + 537.37A + 453.70B + 360.77C + 554.86D - 203.72AB - 775.98AC - 369.16AD - 643.83BC - 478.35BD - 806.61CD + 3448.89ABD \quad (1)$$

Polydispersity Index (PdI) (Y2) = + 13.41A + 15.97B + 27.79C + 28.65D – 59.16AB – 78.93AC – 80.12AD – 85.13BC – 86.29BD – 114.92CD + 138.23ABC + 143.03ABD + 186.97ACD + 202.18BCD (2)

Table 2 shows the 20 formulations with different percentages of four independent factors for the D-optimal MD and their dependent responses. The tables show the actual particle size and PdI values versus the corresponding predicted values to verify the quality and reliability of the obtained model. Based on the results, the actual values were generally close to the predicted values, indicating exceptional fitness of the model generated by the D-optimal mixture design.

The study performed ANOVA to predict the significance of model fitting. The statistically significant parameters for both responses (particle size and PdI), viz., coefficient of determination (R^2), adjusted coefficient of determination (R^2_{adj}), adequate precision, F-value, p-value, lack of fit, and coefficient of estimation, are listed in Table 3. As can be seen, data for both responses fitted closely to the special cubic model using the Design-Expert software. While it is true that in **Table 3(a)** for particle size, only two specific interaction terms (AC and ABD) reach statistical significance ($p < 0.05$), this does not undermine the overall influence of the selected parameters (jojoba oil [A], grapeseed oil [B], Tween 80 [C], and glycerol [D]) on the mixing system. The justification lies in the holistic evaluation of the D-optimal mixture design model, which is appropriate for systems in which responses depend on component proportions rather than on independent factors alone. Results revealed that both models obtained for the response particle size (p-value < 0.001) and PdI (p-value = 0.004) for the OPT-*Pc*E Ne are significant, with the corresponding F-values of 30.57 and 24.20. Notably, the interactive effect of the factors was more pronounced for the former than for the latter in the OPT-*Pc*E Ne. The models' F-values also corroborate the larger values of independent factors seen in Equation 1 (for particle size) compared to Equation 2 (for PdI).

The overall model significance is represented by the special cubic model for particle size, which is highly significant (F-value = 30.57, $p < 0.0001$), indicating that the parameters collectively explain the emulsion process effectively. The high values of R^2 and R^2_{adj} for particle size ($R^2 = 0.9714$, $R^2_{adj} = 0.9396$) and PdI ($R^2 = 0.9813$ $R^2_{adj} = 0.9407$) with higher lack of fit ($p > 0.05$) for both of them, verified desirable suitability of the fitted models to predict values of the particle size and PdI of the *Pc*E-Ne as a function of the amounts of oil and surfactant. This means the model explains over 97% of the variance in the responses (particle size and PdI) (**Table 3**).

Table 2. D-optimal mixture design and response values for the OPT-*Pc*E Ne formulation process

Independent Variables					Dependent Responses			
Run	JO(A) (%)	GSO (B) (%)	T80© (%)	GLY(D) (%)	Particle size (nm)		PdI	
					Pred.	Act.	Pred.	Act.
1	6.25	43.75	14.06	35.94	256.23	253.00	0.19	0.19
2	18.75	34.37	7.81	39.06	393.46	399.30	0.40	0.40
3	18.75	31.25	14.06	35.94	271.69	268.50	0.24	0.22
4	6.25	34.38	14.06	45.31	240.36	222.90	0.18	0.16
5	9.38	40.63	9.38	40.63	325.08	366.10	0.24	0.24
6	12.50	37.50	4.69	45.31	521.23	526.40	0.47	0.47
7	18.75	31.25	4.69	45.31	454.47	485.50	0.32	0.33
8	12.50	37.50	14.06	35.94	247.32	244.10	0.22	0.22
9	10.94	43.75	9.38	35.94	312.34	321.90	0.29	0.29
10	14.07	31.25	14.06	40.63	244.37	245.20	0.20	0.21
11	15.62	43.75	4.69	35.94	439.67	416.00	0.39	0.40
12	18.75	31.25	14.06	35.94	271.69	273.10	0.24	0.26
13	15.62	43.75	4.69	35.94	439.67	460.70	0.39	0.37
14	6.25	39.07	9.38	45.31	280.59	280.00	0.29	0.30
15	6.25	34.38	14.06	45.31	240.36	252.90	0.18	0.19
16	14.07	31.25	9.38	45.31	317.08	321.90	0.30	0.29
17	18.75	31.25	4.69	45.31	454.47	418.00	0.32	0.31
18	6.25	43.75	4.69	45.31	379.90	373.40	0.27	0.29
19	6.25	43.75	4.69	45.31	379.90	388.00	0.27	0.26
20	6.25	39.07	14.06	40.63	226.34	239.30	0.20	0.19

* JO = Jojoba Oil, GSO = Grapeseed oil, T80 = Tween 80, GLY = Glycerol, PdI = Polydispersity Index

Table 3. ANOVA and regression coefficient for (a) particle size and (b) PdI of the OPT-*Pc*E Ne

(a) Particle Size, Y_1			
Source	**Coefficient estimate**	**F value**	***p*-value**
Model	-	30.57	< 0.0001*
Linear Mixture	-	92.97	< 0.0001*
AB	-203.72	0.44	0.5244
AC	-775.98	6.45	0.0318*
AD	-369.16	0.98	0.3484
BC	-643.83	3.61	0.0900
BD	-478.35	1.57	0.2414
CD	-806.61	4.41	0.0652
ABD	3448.89	12.97	0.0057*
Lack of Fit		0.25	0.9001^{ns}
R^2			0.9714
R^2_{adj}			0.9396
R^2_{pre}			0.8457
Adeq. Precision			17.5823
ns – not significant		** – significant*	
(b) Polydispersity Index, Y_2			
Source	**Coefficient estimate**	**F-value**	***p*-value**
Model	-	24.20	0.0004*
Linear Mixture	-	77.81	< 0.0001*
AB	-59.16	10.48	0.0177*
AC	-78.93	10.74	0.0169*
AD	-80.12	11.18	0.0155*
BC	-85.13	10.44	0.0179*
BD	-86.29	10.83	0.0166*
CD	-114.92	10.93	0.0163*
ABC	138.23	10.53	0.0176*
ABD	143.03	11.18	0.0155*
ACD	186.97	11.05	0.0159*
BCD	202.18	10.74	0.0169*
Lack of Fit	-	0.25	0.5344^{ns}
R^2			0.9813
R^2_{adj}			0.9407
Adeq. Precision			17.4953

ns – not significant ** – significant*

This determination is based on standard statistical criteria for regression models, where R^2 measures how well the independent variables (jojoba oil, grapeseed oil, T80, and glycerol) account for variability in the dependent variables. High R^2 values close to 1 suggest the model reliably predicts outcomes with minimal unexplained variance, which is particularly desirable in formulation optimization to ensure reproducibility and accuracy. In fact, in pharmaceutical and cosmetic formulation studies using response surface methodologies (similar to D-optimal designs), R^2 values > 0.70–0.80 are typically deemed acceptable, whereas values > 0.90 (as in our study) reflect robust model performance with minimal unexplained variation.

As can be seen, the adjusted R^2 values (particle size: 0.9396; PdI: 0.9407) are lower than the corresponding R^2 values (0.9714 and 0.9813) because R^2_{adj} penalizes for the number of predictors in the model. This difference is expected in multiple regression and reflects the principle that R^2 always increases when terms are added, while adjusted R^2 increases only if the new terms improve the model more than expected by chance [24]. For particle size, the 0.0318 difference arises primarily from five non-significant two-factor interaction terms (AB, AD, BC, BD, CD with $p>0.05$) that contribute minimally to predictive ability. These terms were retained to maintain model hierarchy, as the three-factor term ABD ($p=0.0057$) was significant. For PdI, the slightly larger difference (0.0406) reflects the larger number of model terms (13) relative to runs (20), although all terms in this model are statistically significant ($p<0.05$). The differences between R^2 and

R^2_{adj} in both models are well below the acceptable threshold of 0.2 reported in the literature [22], confirming that our models are not overparameterized. Additional diagnostics, including adequate precision (>17 for both responses), non-significant lack-of-fit (p >0.05), and predicted R^2 values, further support model adequacy for navigating the design space and predicting optimal formulations.

Likewise, the statistical data showed that the p - value of the special cubic model was less than 0.05 (significantly different) [12, 25]. All R^2 and adjusted R^2 values for the responses were similar (the difference between R^2 and adjusted R^2 was < 0.2). The outcome seen here indicated that the relationship between Y_1 and Y_2 (Particle size and PdI) and independent factors fitted well with the special cubic model. In summary, the selected parameters adequately explain the emulsion process, as evidenced by the model's strong statistical fitness and predictive power (predicted $R^2 = 0.8457$). Our focus on only two significant interactions overlooks the dominant linear mixture effects and overall model performance, which are standard in mixture designs for capturing blended system dynamics [25].

Figure 1 substantiates the good correlation between the predicted *versus* actual values obtained in this study. This was apparent from the normally distributed values, in which the linearity of the plot indicated the absence of outliers. Thus, the model could reliably correlate the assessed factors and the two responses and predict the smallest particle size and PdI of the best *Pc*E-Ne. Equally, the lack of fit ($p > 0.05$) for the particle size and PdI at 0.9001 and 0.5344 was insignificant in relevance to the pure error. This means that the obtained model fits well with the predicted outcome or the experimental design. Moreover, the high values of adequate precision for both responses, particle size = 17.5823 and PdI = 17.4953, which measure the signal-to-noise ratio for both responses (**Table 3**), indicated the models' adequacy to navigate the design space to predict the formulation of a good and stable *Pc*E-Ne.

The model terms AC and ABD were considered significant for particle size, as their p-values were <0.05. The positive and negative signs preceding all terms in Equations (1) and (2) refer to their synergistic and antagonistic impact on the responses in the optimization experiment. The amount of jojoba oil (A) impacted particle size the most, while the amount of glycerol (D) affected the PdI. The Box-Cox plot illustrates the normality of the residual distribution, with the lowest point indicating the optimal lambda value, which specifies the power of the transformation [25]. In this study, the Box-Cox suggested that -0.5 was the best Lambda value for the transformation of the inverse square root for the normally distributed plots for particle size. In contrast, the Lambda value was equal to 1 for PdI, conveying that transformations were unnecessary, and the residuals were normally distributed (**Figure 2**).

D-optimal optimization analysis: Particle size

In this work, contour plots (2D) were constructed to assess the effects of four factors on the responses, particle size, and PdI of *Pc*E-Ne. As reported in the above section, only the interaction term ABD yielded an F-value of 12.97 and a p-value of 0.0057, indicating a significant impact on lowering the particle size of *Pc*E-Ne. Therefore, the subsequent section only discusses the interactions for ABD at constant T80 (T80) composition. **Figure 3** demonstrates the influence of JO, GSO, and GLY at constant T80 composition, which proves that the interaction of the three factors imparted significant effects (p-value <0.05) on the particle size of the *Pc*E-Ne, respectively.

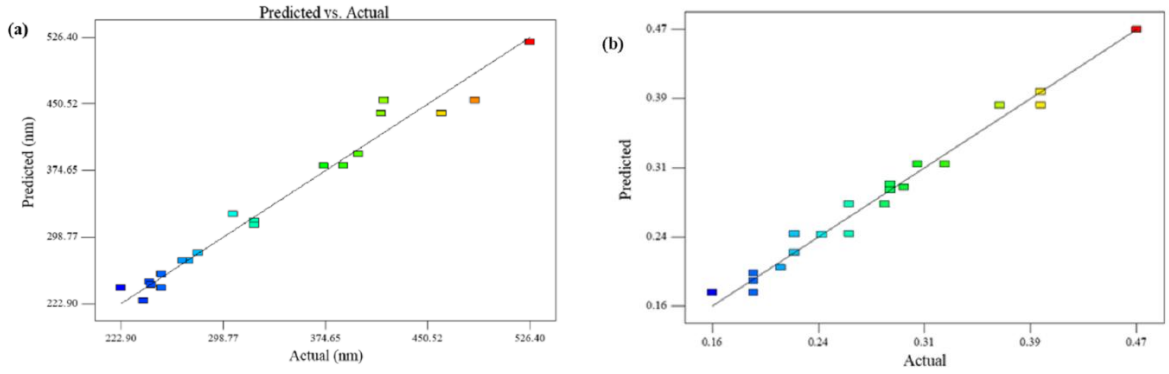

Figure 1. Predicted versus actual plots for (a) Particle size and (b) PdI

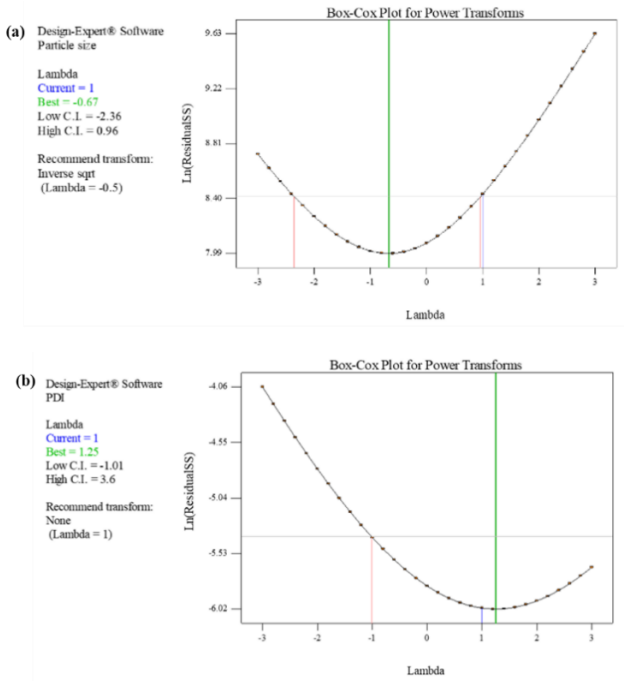

Figure 2. Box-Cox plot for (a) Particle size and (b) PdI

As can be seen, the smallest OPT-PcE-Ne particle size achieved was 276.7 nm, resulting from a formulation comprising approximately 39.84% to 44.9% GSO (B), 6.25% to 7.97% JO (A), and 41.09% to 47.96% GLY (D). A lower oil mixture ratio (approximately 2:3.4, JO: GSO) promoted the formation of smaller particles in the PcE-Ne. Notably, particle size decreased when glycerol concentration was kept below 50%. This outcome is likely due to the unique properties of glycerol, a small, water-soluble cosolvent, which significantly influences the characteristics of aqueous solutions and surfactants in the Ne [20]. Additionally, a higher T80 concentration further contributed to smaller particles, consistent with previous findings that increased surfactant levels help stabilize the interfacial space and reduce particle size [19]. Therefore, it can be construed that the synergistic interaction between glycerol (41.09% to 47.96%) and T80 (9.37%) in the formulation led to smaller PcE-Ne droplets.

This study incorporated glycerol into the aqueous phase to reduce the surfactant content in the resultant OPT-PcE-Ne droplets, aiming to minimize sensitivity in certain individuals to formulations with high surfactant concentrations. The approach taken here mirrors the strategy used in optimizing microemulsion formulations containing solubilized vitamin A [26]. Another notable factor in the OPT-PcE-Ne formulation is the need for a lower JO composition (6.25 to 7.97%) to achieve the smallest PcE-Ne droplets. This outcome was expected since JO is a relatively viscous oil. However, its inclusion was intentional due to its hypoallergenic, moisturizing properties, easy skin penetration, and potent anti-inflammatory effects. Increasing the concentration of JO could significantly alter the physicochemical properties and interfacial tension of the aqueous solution, potentially increasing the mixture's viscosity and density. This observation aligns with earlier reports showing an increase in droplet size when higher glycerol concentrations (another viscous component) were added to the formulation [20]. Consequently, a fixed composition of T80 at 9.375% and a low glycerol concentration were found to favor smaller average particle sizes in the OPT-PcE-Ne. This outcome highlights the importance of using a moderate T80 concentration to reduce the PcE droplet size in the OPT-PcE-Ne formulation, especially when JO and glycerol are components of the nanoemulsion.

Literature has shown that smaller average particle sizes in nanoemulsions (Ne) contribute to greater colloidal stability, suggesting that the stability of PcE-Ne systems is more influenced by Brownian motion than gravitational forces. Also, a colloidal system dominated by Brownian motion is less prone to issues such as creaming, sedimentation, and coalescence [26]. Thus, particle size plays a crucial role in the D-optimal design (MD) for formulating the most stable PcE-Ne. This technique is widely used to evaluate nanoemulsion stability, as smaller particle sizes help prevent destabilizing phenomena such as flocculation and coalescence [27].

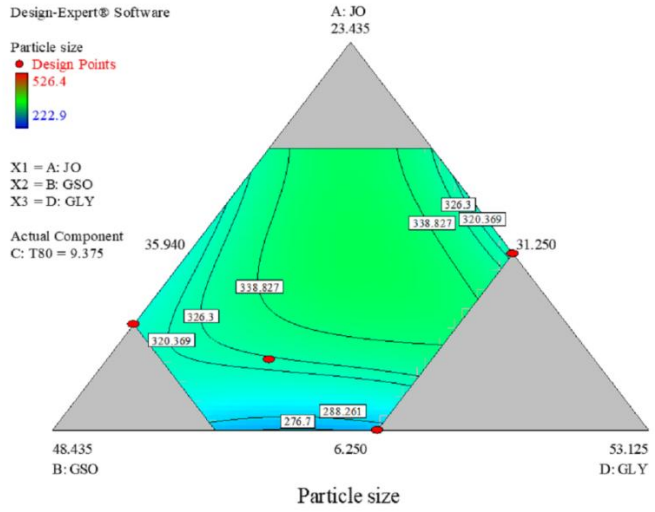

Figure 3. The 2D surface plot shows the interaction effects among three factors: (A) jojoba oil, (B) grapeseed oil, and (D) glycerol, on the response variable, particle size

D-optimal optimization analysis: Polydispersity Index (PdI)

The PdI (polydispersity index) is a key indicator of droplet size distribution in nanoemulsions [28] and is essential for determining the quality of a nanoemulsion. The PdI value reflects the uniformity of droplet distribution, with values approaching zero indicating a monodispersed system, while values closer to one (1) indicate polydispersity [28]. PdI values greater than 0.7 suggest a wide particle size distribution, indicating a polydispersed system, which is unsuitable for DLS analysis. An ideal monodispersed system typically has a PdI value below 0.25 [28]. **Figure 4** illustrates 2D contour plots of the significant mutual interactions between JO (A), grapeseed oil (GSO)(B), T80 (C), and glycerol (D) in terms of PdI. As shown in **Table 3(b)**, the p-values for all mutual interactions, ABC, ABD, CBD, ACD, and BCD, were statistically significant (p-value <0.05), conveying that the tested factors and their ranges played a substantial role in reducing the PdI of the *Pc*E-Ne. Therefore, the following paragraphs explore the general manner of their interactions to favorably reduce the PdI of the best PcE-Ne.

The results showed that the p-value for ABC was 0.0176 (**Table 3b**), with a constant GLY composition of 40.625%, indicating that the three factors significantly influenced the PdI value of the PcE-Ne. As shown in the contour plot in **Figure 4(a)**, the lowest PdI (0.19) was achieved with a low composition of JO (6.25 to 8.83%), suggesting that a reduced presence of the viscous JO contributed to the formation of a monodispersed PcE-Ne. The PdI reached its minimum (0.19) and produced a monodispersed PcE-Ne when a smaller amount of JO (6.25%) was combined with moderate compositions of T80 and GSO. The liquid wax characteristic of JO, attributed to its linear ester composition and 40 to 60% oil content, differentiates it from other vegetable oils. Despite this, JO was a critical component of our formulation, offering superior functional cosmetic properties compared with triglycerides such as GSO [29]. In contrast, the optimal GSO composition for achieving the lowest PdI (0.19) in the PcE-Ne was between 41.46 and 44.9%. Similarly, the lowest PdI was attained when T80 compositions were set between 10.93 and 14.06%. The non-ionic T80 used in the PcE-Ne formulation acted as a ripening inhibitor, enhancing the stability of the PcE-Ne system. T80 stabilizes the system by preventing droplet coalescence through short-range repulsive forces, including steric overlap, hydration, and thermal-fluctuation interactions [30]. In summary, the proportion of JO and GSO in the PcE-Ne mixture had a significant impact on the dispersivity of the PcE droplets (p-value 0.0176). A lower JO:GSO ratio, along with a moderate T80, was the most favorable combination (**Figure 4a**).

A similar outcome was observed in Figures 4b-c when the T80, GSO, and JO compositions were set at mid-range values (9.375%, 37.5%, and 12.5%, respectively). Moderate compositions of GSO and GLY (less than 50%) resulted in the lowest PdI (0.19) for the OPT-PcE Ne. GLY plays a crucial role in influencing the emulsion's interfacial tension, optimal curvature, and the solubility properties of both ionic and non-ionic surfactants, which in turn improve the molecules' monodispersity in the aqueous phase of the PcE Ne, as described in earlier literature. This water-soluble GLY, as a co-solvent, appears to favorably

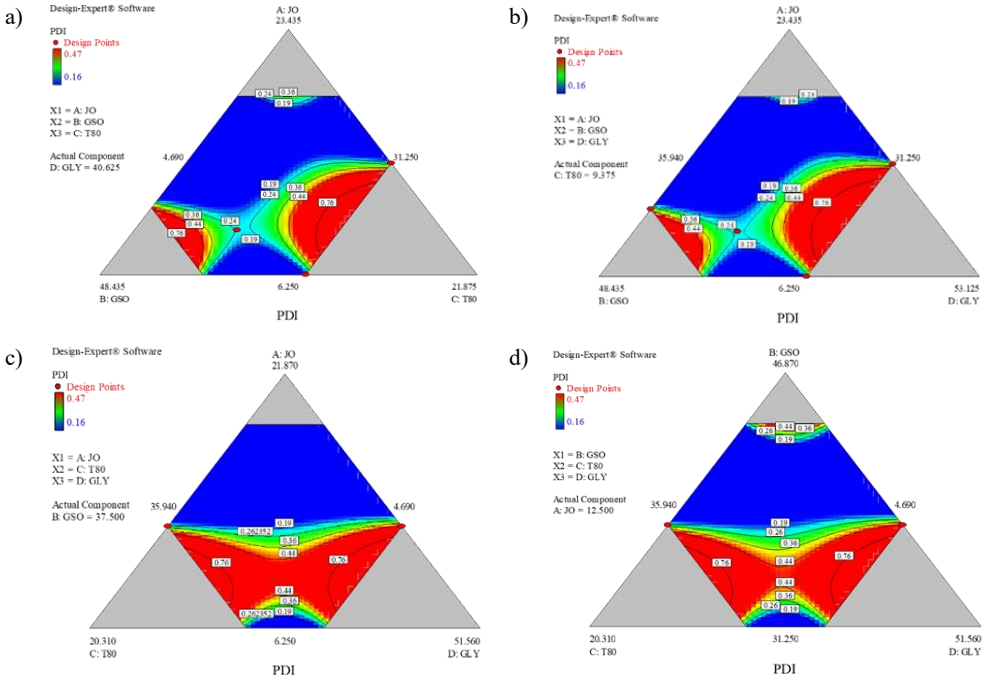

Figure 4. The 2D contour plots show the mutual interaction between four factors, jojoba oil (A), grapeseed oil (B), T80 (C), and glycerol (D), for the response, PdI

alter the core physicochemical properties, such as density, viscosity, and interfacial tension, thereby enhancing the stability of the OPT-PcE Ne [20]. The outcome seen here thus corresponds well with the low PdI value of the PcE-Ne when T80 was mixed with other excipients in the formulation. Based on the plots in Figures 4a-d, it can be concluded that the lowest PdI value for OPT-PcE-Ne (0.19) is achieved when all four components are set at their mid-range values. However, JO, which forms the minor component, is the exception in the most monodispersed OPT-PcE Ne formulation (PdI 0.19). Thus, this study successfully employed the D-optimal MD experiment to identify the optimal formulation for a stable OPT-PcE Ne, characterized by the smallest particle size (276.7 nm) and the lowest PdI (0.19).

Model verification

The predicted response values were verified against the ideal values of the independent variables after completing the optimization experiment by comparing them with the experimental values (**Table 4**). Thus, for model verification, the formulation with the highest desirability value (approaching 100%) was selected from the D-optimal design space. This formulation, comprising 6.25% JO, 38.21% GSO, 14% T80, and 41.48% GLY, represented the predicted optimum for simultaneously minimizing both particle size and PdI. The predicted responses were then experimentally validated in triplicate, and the percentage prediction error (PPE) was calculated to assess model accuracy. This approach of verifying the optimal point, rather than random points, is standard in mixture design optimization as it directly confirms that the model successfully identified the true formulation optimum [14,20]. The predicted percentage error (PPE) for particle size (6.04%) and PdI (8.02%) of OPT-PcE-Ne were both below 10%, confirming the model's acceptability in identifying the best composition of PcE-Ne, with the smallest particle size and the lowest PdI.

The outcome observed in this study is similar to that of a study by Yahya et al., which employed a D-optimal mixture design to optimize a nanoemulsion system using pineapple peel extract, with independent variables including olive oil, grapeseed oil, Tween 80, and water. The model verification step demonstrated satisfactory agreement between predicted and experimental values, with the percentage prediction error (PPE) for both droplet size and the polydispersity index (PDI) below 10% [12]. This finding is highly consistent with our technical article, where the PPE for particle size (6.04%) and PdI (8.02%) were also below 10%, confirming the model's acceptability. Likewise, Sulaiman et al. used a D-optimal mixture design to optimize a nanoemulsion system containing *Clinacanthus nutans* leaf extract for transdermal delivery. The goal was to determine the optimal levels of five independent variables to minimize average droplet size. The model verification showed excellent agreement between the predicted

Table 4 Verification model for OPT-*Pc*E-Ne formulation

Variables (%)				Particle Size		PPE	PDI		PPE
JO(A)	**GSO(B)**	**T80(C)**	**GLY(D)**	(Pred)	(Act)	(%)	(Pred)	(A)	(%)
6.25	38.21	14	41.48	225.6	240.1	6.04	0.20	0.21	8.02

and actual values, with a residual standard error (RSE) of only 2.61% [23]. Thus, these studies collectively reinforce the robustness of the D-optimal mixture design approach for developing stable nanoemulsions with desirable physicochemical properties for cosmeceutical applications, and they validate the use of low prediction errors as a key indicator of model reliability.

Characterizations of the optimized *Pouteria campechiana* pulp extract nanoemulsion: Organoleptic evaluation

Organoleptic qualities, those perceived by human senses, are critical for consumer acceptance of a topical product. Factors such as color, visual homogeneity, texture (feel), and consistency influence a user's willingness to apply the product regularly [31]. The optimized formulation (OPT-PcE-Ne) was subjected to a battery of tests to assess its suitability for use as a topical product. These evaluations can be broadly categorized into assessments of its consumer-acceptable sensory attributes and its physicochemical stability. In this study, the OPT-PcE-Ne was assessed for these properties. The formulation remained a creamy white color with no change over 90 days, indicating good physical stability against oxidation or browning. It exhibited uniform consistency and good spreadability, leaving no white cast or residue upon application. A mildly greasy feel was noted, but the formulation was readily absorbed, consistent with nano-sized droplets facilitating penetration. These favorable sensory characteristics suggest that the OPT-PcE-Ne would be well-received by consumers [32].

Organoleptic evaluation

While organoleptic properties address consumer appeal, the formulation's long-term shelf life depends on its physical stability, assessed by measuring the zeta potential. Zeta potential quantifies the electrostatic repulsion between dispersed droplets, a key indicator of a colloidal system's resistance to coalescence and aggregation [33]. The magnitude of the zeta potential is a reliable early indicator of the electrokinetic stability of a colloidal system and correlates with both short- and long-term stability of the formulation [34]. A high magnitude (either positive or negative) indicates strong repulsive forces that prevent droplet fusion [17].

Figure 5 illustrates the zeta potential distribution for the OPT-PcE-Ne, which was measured at -32.6 ± 0.5 mV. This value, which falls outside the typical agglomeration threshold of ±30 mV, confirms that the formulation possesses a strong negative surface charge. This highly negative charge creates a sufficient energy barrier between droplets, preventing coalescence and ensuring long-term stability against phenomena like creaming and phase separation [35]. This electrostatic stabilization is primarily attributed to the polyoxyethylene groups of the non-ionic surfactant T80, which can generate a negative surface potential through specific interactions at the oil-water interface [36,37]. Together, these analyses provide a holistic view of the formulation's readiness for further development. The zeta potential analysis provides the scientific evidence that the formulation is physically stable and will maintain its integrity over time. The organoleptic evaluation provides the practical evidence that the formulation is aesthetically pleasing and suitable for real-world topical application. A cosmeceutical product must excel in both domains to be successful [34].

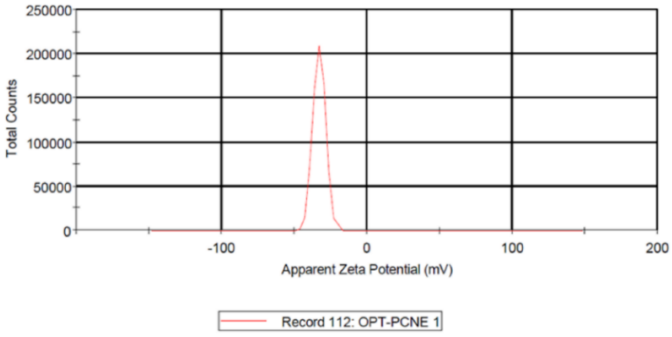

Figure 5. Graph illustrating the zeta potential of the OPT-*Pc*E-Ne

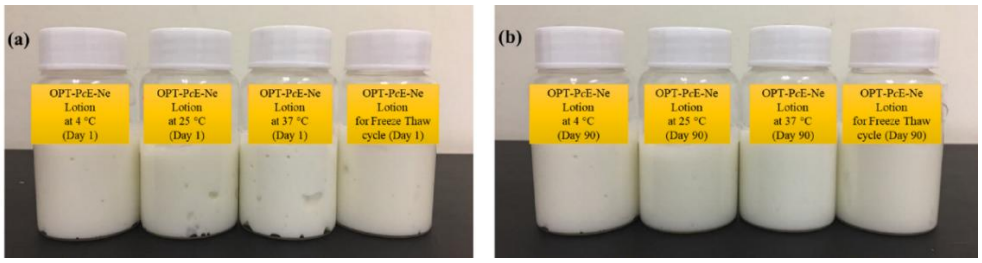

Figure 6. Physical appearances of the OPT-*Pc*E-Ne samples for (a) Day-1 and (b) Day-90

Table 5. Summary of stability of the OPT-*Pc*E-Ne samples stored at 4 °C, 25 °C, and 37 °C.

Day (s)	15			30			45			60			90		
Temperature (°C)	4	25	37	4	25	37	4	25	37	4	25	37	4	25	37
Stability	√	√	√	√	√	√	√	√	√	√	√	√	√	√	√

pH

The pH of human skin varies from pH 4−6 according to the area of the skin and the individual's age. Hence, an aqueous phase pH value between 4−7 is preferred for a topical formulation [13] to avoid disruption of the acid mantle. In this study, the average pH of the tested OPT-*Pc*E-Ne samples was found to be pH 4.81±0.02. This proves that the optimized formulation was suitable for topical usage. This value aligns with the human skin's natural acid mantle (pH 4–6, varying by age and area), preventing disruption that could lead to irritation or microbial growth. In vivo skin compatibility studies, the pH value alone, measured using a calibrated pH meter as described in our methodology, provides sufficient scientific evidence that the formulation is non-irritating with respect to pH. In fact, this is standard practice in preliminary cosmetic formulation studies [38]. Also, since the pH system of OPT-*Pc*E-Ne (4.81±0.02) falls on the lower end of the recommended pH spectrum for topically applied emulsions, the zeta potential of the Ne could likely increase as the pH decreases. It is vital to mention here that these values apply to the entire oil droplet/precipitate particle system [38]. This study considered this matter, as it has been documented that the zeta potential magnitude of Ne is lowest at very low pH and highest at moderate pH [39,44].

Thermodynamic stability: Temperature and freeze-thaw test

Stability is an important aspect of formulating a good nanoemulsion. Hence, stability tests are crucial for their predictive capacity to gauge the stability of newly formulated nanoemulsions under various climatic conditions [40]. In this study, OPT-PcE-Ne samples were subjected to three parallel long-term storage conditions: refrigerated (4°C ± 2°C), room temperature (25°C ± 2°C), and accelerated (45°C ± 2°C) for up to 90 days. The selection of these temperatures follows ISO/TR 18811:2018 guidelines for cosmetic stability testing [44]. Refrigerated conditions assess cold-storage stability; room temperature represents typical consumer-use conditions; and elevated temperature (45°C) serves as an accelerated condition to predict long-term shelf life and ensure suitability for tropical climates [12]. As shown in **Table 5**, no phase separation, turbidity, creaming, or cracking was observed in any sample across all temperatures throughout the 90-day period. After 90 days of storage, the OPT-PcE-Ne remained relatively stable with no visible changes in the emulsions' color and consistency, as shown in **Figure 6**. This exceptional stability is likely a consequence of the formulation's highly negative zeta potential (-32.6 ± 0.5 mV), which provides strong electrostatic repulsive forces preventing droplet coalescence [33].

The destabilization of o/w nanoemulsions during freeze-thaw cycles is associated with changes in physicochemical attributes, including fat deposition, ice formation, interfacial phase transitions, and alterations in conformational, chemical, or electrostatic interactions within the interfacial layer of the colloidal system [46]. **Table 6** indicates the exceptional stability of the OPT46-PcE-Ne samples after five consecutive cycles of freeze-thaw at 4 °C and 40 °C, which agrees well with its satisfactory zeta potential (– 32.6 mV). The OPT-*Pc*E-Ne's ability to resist phase separation may be due to the hydrophilic head groups of T80. The surfactant formed a stearic barrier at the oil/water interface, reducing effective collisions between OPT-*Pc*E-Ne droplets, especially at higher temperatures (25 °C and 40 °C). This precluded the OPT-*Pc*E-Ne destabilization by coalescence [12]. The use of XG as the thickener was another possible stabilizing factor in the OPT-*Pc*E-Ne

Table 6. Summary of freeze-thaw stability for OPT-*Pc*E-Ne

Stability Test	Freeze-Thaw (cycles)									
	1		2		3		4		5	
Temperature (°C)	4	40	4	40	4	40	4	40	4	40
Stability	√	√	√	√	√	√	√	√	√	√

formulation. The action of XG increases the OPT-*Pc*E-Ne's viscosity, thus delaying coalescence in the continuous phase and reducing droplet collision. The above results thus collectively supported the well-formulated and stable OPT-*Pc*E-Ne. Also, the nanoemulsion's good homogeneity was expected to be retained under varying storage temperatures.

Centrifugation and mechanical vibration test

An accelerated test is essential to evaluate the stability of the newly formulated nanoemulsion (Ne) and to predict its shelf life under normal storage conditions. The centrifugation test provides a direct measure of Ne stability by accelerating phase separation, thereby increasing the rate of creaming or sedimentation [12]. The results of this study align with those of Parveen et al. [42], who reported an optimal formulation with a particle size of 41.22 ± 0.00314 nm and a PdI of 0.165. This can be attributed to the presence of non-ionic polyoxyethylene sorbitan esters, such as Tween 80 (T80), which effectively lower the surface tension between active component particles. This reduction in surface tension prevents coalescence and delays the rapid release of bioactive ingredients from the nanoemulsion [18,42].

Likewise, the favorable PdI value of 0.19 observed in the OPT-PcE Ne may be due to the non-polar, unsaturated tails of T80. This is due to the unsaturated tails of the emulsifier, which promote loose molecular packing, enabling the spontaneous formation of ultrafine PcE-Ne droplets at the oil–water interface. The ideal ratio between the cross-sectional areas of T80's hydrophobic tail and hydrophilic head group determines its molecular geometry, thereby forming a stable monolayer curvature during emulsification. Similar behavior has been reported in studies using T80 as a surfactant [36]. Additionally, the conductivity values further confirm that the system is oil-in-water (o/w), as o/w emulsions typically exhibit conductivity > 0.00 µS/cm due to their aqueous continuous phase. In contrast, oil phases are non-conductive, yielding values close to 0.00 µS/cm [43, 44]. In this study, the OPT-PcE-Ne was identified as an oil-in-water (o/w) nanoemulsion based on its conductivity value of 0.22 µS/cm. This relatively low conductivity is attributed to the formulation's limited water content (33% v/w), consistent with findings by Huang et al., who reported near-zero conductivity for o/w emulsions with high oil content (>30% v/v). Although the continuous phase is aqueous, the elevated oil content used in the formulation reduces overall conductivity. In Huang's study, emulsions were confirmed to be o/w systems when the oil mass fraction exceeded 40% [44]. Similarly, the OPT-PcE-Ne, containing 32% (v/v) oil, is a borderline o/w system, which explains its near-zero conductivity. Conductivity increased slightly as water content rose to 33% of the total volume. Since the external phase primarily dictates emulsion conductivity, verifying it is essential for confirming the system type. Oil-in-water systems are particularly desirable in cosmetic formulations due to their cost-effectiveness and favorable sensory attributes [23], underscoring the importance of conductivity testing for the OPT-PcE-Ne.

Rheology study

An emulsion's composition plays a key role in its rheological behavior, given its profound impact on droplet long-term stability and on the type of interfacial interactions between droplets. Rheological data also offers insight into Ne's physicochemical and sensory properties [12]. In this study, the rheological behavior of OPT-PcE-Ne was assessed, as these findings impact the decision on the nanoemulsion's applicability and consumer acceptance. Figure 7 revealed that the OPT-*Pc*E-Ne exhibited Bingham plastic behavior, as evidenced by its relatively high viscosity. This is because yield stress is required for a Bingham plastic fluid to flow. Before this fluid can flow, it must be subjected to a force exceeding the yield stress [12,45].

The Bingham plastic fluid of the OPT-*Pc*E-Ne showed that the system exhibits Newtonian behavior once the yield stress is reached. This flow behavior guides engineers in selecting the correct nozzle flow rate for large-scale preparation of OPT-*Pc*E-Ne. Then again, the plastic nature of OPT-*Pc*E-Ne indicates its low resistance to flow under high shear conditions. The outcome was consistent with the favorable rheological characteristics of OPT-PcE-Ne for topical application to the skin. A plastic, topically applied cosmetic Ne system is commonly applied to the skin in layers [36]. Notably, many marketed cosmeceutical Nes exhibited plastic behavior similar to that of OPT-*Pc*E-Ne [46].

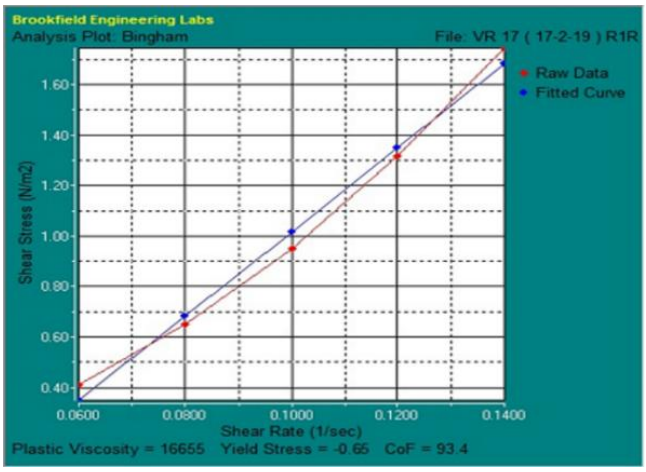

Figure 7. Bingham model coupled with the OPT-*Pc*E-Ne

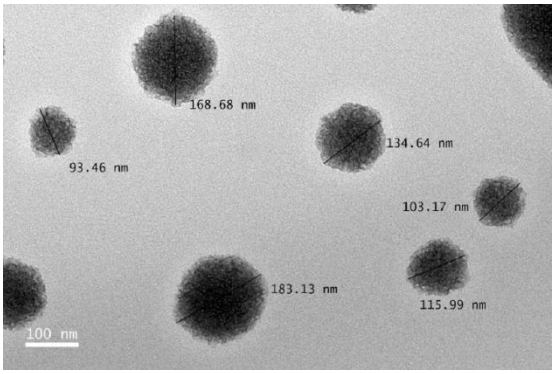

Figure 8. TEM micrograph of OPT-*Pc*E-Ne droplets

Particle morphology: TEM

Microscopic characterization of a newly developed Ne is crucial for validating the average droplet size in the colloidal system. The technique is also a secondary test that confirms the average particle size and degree of dispersity from earlier DLS analysis. In this study, conventional negative staining with uranyl acetate was performed before TEM analysis to identify the dehydrated droplet shells stabilized by the surfactant. The TEM micrograph (**Figure 8**) revealed that the OPT-PcE-Ne particles were spherical and homogeneously distributed. This observation aligns well with the DLS results, which indicated an average particle size of 240.1 nm and a PdI of 0.19, suggesting moderate monodispersity. TEM analysis showed particle sizes ranging from 93.46 to 183.13 nm. A few larger droplets, indicative of minor Ostwald ripening, were also observed. Notably, the corresponding micrograph confirmed the absence of particle aggregation, further supporting the DLS findings (~200 nm). Likewise, the spherical morphology and narrow size distribution were direct reflections of the favorable characteristics of the OPT-PcE-Ne formulation, thereby contributing to its stability by reducing the risk of creaming and sedimentation events [12].

Conclusion

This study demonstrated that a fitted special cubic model using D-optimal mixture design (MD) effectively identified the optimal composition of OPT-PcE-Ne based on four key components: jojoba oil (JO, A), grapeseed oil (GSO, B), Tween 80 (T80, C), and glycerol (GLY, D). The model responses pertaining to droplet size and polydispersity index (PdI) were statistically validated by ANOVA, showing significant p-values (<0.05), non-significant lack-of-fit values (droplet size = 0.9001, PdI = 0.5344), and high coefficients of determination (R^2: droplet size = 0.9714, PdI = 0.9813). The optimized formulation consisted of 6.25% JO, 38.21% GSO, 14% T80, and 41.48% GLY, yielding a minimal droplet size (240.1 ± 0.81 nm) and low PdI (0.21 ± 0.017). The experimental values closely matched the predicted ones, with a percentage prediction error (PPE) below 10%. Our organoleptic and characterization assessments further confirmed the formulation's physical stability and suitability for topical

application. Overall, the results of this study support the potential of OPT-PcE-Ne as an effective delivery system for nature-based cosmetic products.

Acknowledgement
The authors would like to thank the Department of Chemistry, Faculty of Science, Universiti Teknologi Malaysia, for their facilities. They would like to thank the Collaborative Outreach for International Research Networking (Connect 2025) and the Research and Service Institutions of Udayana University. The Contract Number B/229.145/UN14.4.A/PT.01.03/ 2025, dated April 28, 2025.

References

1. de Lanerolle, M., Priyadarshani, A., Sumithraar achchi, D., and Jansz, E. (2009). The carotenoid s of *Pouteria campechiana* (Sinhala: ratalawulu) . *Journal of the National Science Foundation of Sri Lanka*, 36(1), 95.
2. Pino, J. A. (2010). Volatile compounds from fruits of *Pouteria campechiana* (Kunth) Baehni. *Journal of Essential Oil Bearing Plants*, 13, 326 –330.
3. Granados-Vega, K., Evangelista-Lozano, S., Esc obar-Arellano, S., Rodríguez-García, T., Pérez-Barcena, J., and Cruz-Castillo, J. (2023). Harvest season and morphological variation of canistel (*Pouteria campechiana*) fruit and leaves collected in different zones of Mexico. *Horticulturae*, 9(11), 1214.
4. Ma, J., Yang, H., Basile, M. J., and Kennelly, E. J. (2004). Analysis of polyphenolic antioxidants from the fruits of three *Pouteria* species by selected ion monitoring liquid chromatography–mass spectrometry. *Journal of Agricultural and Food Chemistry*, 52, 5873–5878.
5. Murillo, E., Meléndez-Martínez, A. J., and Portugal, F. (2010). Screening of vegetables and fruits from Panama for rich sources of lutein and zeaxanthin. *Food Chemistry*, 122, 167–172.
6. Lee, J., Jung, E., Lee, J., Huh, S., Kim, J., Park, M., So, J., Ham, Y., Jung, K., and Hyun, C. G. (2007). Panax ginseng induces human Type I collagen synthesis through activation of Smad signaling. *Journal of Ethnopharmacology*, 109, 29–34.
7. Laguna, C., De La Cuadra, J., Martín-González, B., Zaragoza, V., Martínez-Casimiro, L., and Alegre, V. (2009). Allergic contact dermatitis to cosmetics. *Actas Dermo-Sifiliográficas (English Edition)*, 100, 53–60.
8. Ustun Argon, Z., Celenk, V. U., and Gumus, Z. P. (2020). Chapter 5 - Cold pressed grape (*Vitis vinifera*) seed oil. In M. F. Ramadan (Ed.), *Cold Pressed Oils* (pp. 39–52). Academic Press.
9. Jog, R., and Burgess, D. J. (2018). Chapter 10 - Excipients used in oral nanocarrier-based formu lations. In A. Barhoum and A. S. Hamdy Makhlouf (Eds.), *Fundamentals of Nanoparticle s* (pp. 279–342). Elsevier.
10. Che Marzuki, N. H., Wahab, R. A., and Abdul Hamid, M. (2019). An overview of nano emulsion: concepts of development and cosmeceutical applications. *Biotechnology & Biotechnological Equipment,* 33, 779–797
11. Yahya, N. A., Wahab, R. A., Hamid, M. A., Ma hat, N. A., Huri, M. A. M., Attan, N., and Hashim, S. E. (2020). Preparation and characterization of acoustically extracted *Ananas comosus* peel powder with enhanced high antioxidant capacity. *Jurnal Teknologi* 82 (4), 14486.
12. Samson, S., Basri, M., Fard Masoumi, H. R., Ab edi Karjiban, R. and Abdul Malek, E. (2016). Design and development of a nanoemulsion system containing copper peptide by D-optimal mixture design and evaluation of its physicochemical properties. *RSC Advances*, 6, 7845-17856.
13. Mazonde, P., Khamanga, S. M., and Walker, R. B. (2020). Design, optimization, manufacture and characterization of efavirenz-loaded flaxseed oil nanoemulsions. *Pharmaceutics*, 12, 797.
14. Okonogi, S., Phumat, P., Khongkhunthian, S., C haijareenont, P., Rades, T., and Müllertz, A. (20 21). Development of self-nanoemulsifying drug delivery systems containing 4-allylpyrocatechol for treatment of oral infections caused by *Candida albicans*. *Pharmaceutics*, 13, 167.
15. Gohil, R., Patel, A., Pandya, T., and Dharamsi, A. (2020). Optimization of brinzolamide loaded microemulsion using formulation by design approach: Characterization and in-vitro evaluation. *Current Drug Therapy*, 15, 37–52.
16. Kumar, N., and Mandal, A. (2018). Thermodynamic and physicochemical properties evaluation for formation and characterization of oil-in-water nanoemulsion. *Journal of Molecular Liquids*, 266, 147–159.
17. Udomrati, S., Cheetangdee, N., Gohtani, S., Surojanametakul, V., and Klongdee, S. (2019). Emulsion stabilization mechanism of combination of esterified maltodextrin and Tween 80 in oil-in-water emulsions. *Food Science Biotechnology,* 29(3), 387-392.
18. Wooster, T. J., Golding, M., and Sanguansri, P. (2008). Impact of oil type on nanoemulsion form ation and Ostwald ripening stability. *Langmuir,* 24, 12758-12765.
19. Saberi, A. H., Fang, Y., and McClements, D. J. (2013). Effect of glycerol on formation, stability and properties of vitamin-E enriched nano emulsions produced using spontaneous emulsification. *Journal of Colloid and Interface*

Science, 411, 105-113.

20. Kumar, N., and Mandal, A. (2018). Thermodynamic and physicochemical properties evaluation for formation and characterization of oil-in-water nanoemulsion. *Journal of Molecular Liquids,* 266, 147–159.
21. Kumar, N., Saif Ali, Kumar, A., and Mandal, A. (2020). Design and formulation of surfactant stabilized O/W emulsion for application in enhanced oil recovery: Effect of pH, salinity and temperature. *Oil & Gas Science and Technology - Rev. IFP Energies Nouvelles*, 75, 72.
22. Sulaiman, I. S. C., Basri, M., Masoumi, H. R. F., Ashari, S. E., and Ismail, M. (2016). Design and development of a nanoemulsion system containing extract of *Clinacanthus nutans* (L.) leaves for transdermal delivery system by D-optimal mixture design and evaluation of its physicochemical properties. *RSC Advances*, 6, 67378–67388.
23. Ma, Q., Davidson, P. M., and Zhong, Q. (2016). Nanoemulsions of thymol and eugenol co-emulsified by lauric arginate and lecithin. *Food Chemistry*, 206, 167–173.
24. Myers, R. H., Montgomery, D. C., and Anderson-Cook, C. M. (2016) in Response Surface Methodology: Process and Product Optimization Using Designed Experiments (4th edition, Wiley).
25. Coles, C. L. J., and Thomas, D. F. W. (1952). The stability of vitamin A alcohol in aqueous and oily media. *Journal of Pharmacy and Pharmacology*, 4, 898–903.
26. Aboofazeli, R. (2010). Nanometric-scaled emulsions (nanoemulsions). *Iranian Journal of Pharmaceutical Research*, 9, 325–326.
27. Danaei, M., Dehghankhold, M., Ataei, S., Hasanzadeh Davarani, F., Javanmard, R., Dokhani, A., Khorasani, S., and Mozafari, M. (2018). Impact of particle size and polydispersity index on the clinical applications of lipidic nanocarrier systems. *Pharmaceutics*, 10, 57.
28. Miwa, T. K. (1971). Jojoba oil wax esters and derived fatty acids and alcohols: Gas chromatographic analyses. *Journal of the American Oil Chemists' Society*, 48, 259–264.
29. Silva, H. D., Cerqueira, M. A., and Vicente, A. A. (2015). Influence of surfactant and processing conditions in the stability of oil-in-water nanoemulsions. *Journal of Food Engineering Part B,* 167, 89–98.
30. Garg, T., Rath, G., and Goyal, A. K. (2015). Comprehensive review on additives of topical dosage forms for drug delivery. *Drug Delivery*, 22, 969–987.
31. Cerda-Opazo, P., Gotteland, M., Oyarzun-Ampuero, F. A., and Garcia, L. (2021). Design, development and evaluation of nanoemulsion containing avocado peel extract with anticancer potential: A novel biological active ingredient to enrich food. *Food Hydrocolloids*, 111, 106370.
32. Bhattacharjee, S. (2016). DLS and zeta potential–what they are and what they are not? *Journal of Controlled Release*, 235, 337-351.
33. Xu, R. (2001). Particle characterization: Light scattering methods. Springer Science & Business Media.
34. Hong, I. K., Kim, S. I., and Lee, S. B. (2018). Effects of HLB value on oil-in-water emulsions: Droplet size, rheological behavior, zeta-potential, and creaming index. *Journal of Industrial and Engineering Chemistry* 67:123-131.
35. Riehm, D. A., Rokke, D. J., Paul, P. G., Lee, H. S., Vizanko, B. S., and McCormick, A. V. (2017). Dispersion of oil into water using lecithin-T80 blends: The role of spontaneous emulsification. *Journal of Colloid and Interface Science,* 487, 52–59.
36. Sis, H., and Birinci, M. (2009). Effect of nonionic and ionic surfactants on zeta potential and dispersion properties of carbon black powders. *Colloids and Surfaces A: Physicochemical and Engineering Aspects*, 341, 60–67.
37. Ali, S. M., and Yosipovitch, G. (2013). Skin pH: from basic science to basic skin care. *Acta Dermato-Venereologica,* 93, 261–269.
38. Lu, G. W., and Gao, P. (2010). Emulsions and microemulsions for topical and transdermal drug delivery. In Handbook of Non-Invasive Drug Delivery Systems (pp. 59–94). Elsevier.
39. Lu, C. L., Li, Y. M., Fu, G. Q., Yang, L., Jiang, J. G., Zhu, L., Lin, F. L., Chen, J., and Lin, Q. S. (2011). Extraction optimisation of daphnoretin from root bark of *Wikstroemia indica* (L.) CA and its anti-tumour activity tests. *Food Chemistry*, 124, 1500–1506.
40. International Standard ISO/TR 18811:2018 - Cosmetics — Guidelines for the stability testing of cosmetic products.
41. Parveen, R., Baboota, S., Ali, J., Ahuja, A., and Ahmad, S. (2015). Stability studies of silymarin nanoemulsion containing Tween 80 as a surfactant. *Journal of Pharmacy and Bioallied Sciences,* 7, 321.
42. Gurpreet, K., and Singh, S. (2018). Review of nanoemulsion formulation and characterization techniques. *Indian Journal of Pharmaceutical*

Sciences, 80, 781–789.

43. Huang, W., Zhu, D., Fan, Y., Xue, X., Yang, H., Jiang, L., Jiang, Q., Chen, J., Jiang, B., and Komarneni, S. (2020). Preparation of stable inverse emulsions of hydroxyethyl methacrylate and their stability evaluation by centrifugal coefficient. *Colloids and Surfaces A: Physicochemical and Engineering Aspects,* 604, 125309.
44. Bhattacharya, l. R. S. and Rhodes, E. (1986). Flow behaviour of oil-in-water emulsions. *The Canadian Journal of Chemical Engineering,* 64, 3-10.
45. Azhar, S. N. A. S., Ashari, S. E., and Salim, N. (2018). Development of a kojic monooleate-enriched oil-in-water nanoemulsion as a potential carrier for hyperpigmentation treatment. *International Journal of Nanomedicine*, 13, 6465–6479.